

Composition measurements related to the Cu₂S/Zn_xCd_{1-x}S heterojunction

L. C. Burton

Citation: [Applied Physics Letters](#) **35**, 780 (1979); doi: 10.1063/1.90976

View online: <http://dx.doi.org/10.1063/1.90976>

View Table of Contents: <http://scitation.aip.org/content/aip/journal/apl/35/10?ver=pdfcov>

Published by the [AIP Publishing](#)

Articles you may be interested in

[Compositional depth profiles of chemiplated Cu₂S/\(Zn,Cd\)S heterojunction solar cells](#)

J. Appl. Phys. **54**, 982 (1983); 10.1063/1.332024

[Cross diffusion of Cd and Zn in Cu₂S formed on Zn_xCd_{1-x}S thin films](#)

J. Appl. Phys. **53**, 1538 (1982); 10.1063/1.330654

[Thinfilm polycrystalline Cu₂S/Cd_{1-x}Zn_xS solar cells of 10% efficiency](#)

Appl. Phys. Lett. **38**, 925 (1981); 10.1063/1.92184

[Analysis of capacitancevoltage measurements on heattreated Cu_{2-x}S/CdS heterojunctions](#)

J. Appl. Phys. **50**, 6406 (1979); 10.1063/1.325731

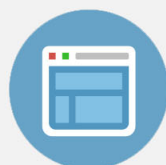
[Zn_xCd_{1-x}S films for use in heterojunction solar cells](#)

Appl. Phys. Lett. **29**, 612 (1976); 10.1063/1.89162

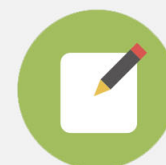


Re-register for Table of Content Alerts

Create a profile.



Sign up today!



The experimental results may indicate the other mechanism of classical stopping of REB electron at the pinch phase; interaction between tightly pinched REB and low- z target. This may be due to the kinetic two stream instability as we proposed before.⁴ The growth rate of this instability is $\delta \sim \omega_p (n_b/n_p) s^{-1}$, where ω_p is electron plasma frequency, and n_b and n_p are the number density of beam and plasma electron, respectively. The condition that $\delta > \frac{1}{2} \nu_{ei}$ must be satisfied to grow this instability to a large amplitude enough to dissipate the beam energy. Here ν_{ei} is the electron-ion collision frequency. This condition gives a rough criteria for when the energy deposition becomes anomalous;

$n_p < 6 \times 10^{15} T_e/z^{2/3} \text{ cm}^{-3}$ for $n_b = 2 \times 10^{14} \text{ cm}^{-3}$, T_e (in eV) is blow-off plasma temperature, and z is ionic charge. For example, in blow-off plasma of $T_e \sim 1 \text{ keV}$,¹¹ the density where the anomalous dissipation can occur is $n_p < 3 \times 10^{18} \text{ cm}^{-3}$ for polyethylene plasma and $n_p < 8 \times 10^{17} \text{ cm}^{-3}$ for Ni plasma. Therefore the collective deposition is effective in low- z plasma.

The experimental results of the measurement of transmitted electron can be interpreted as follows. In the case of a polyethylene target, as the growth rate of the instability increased with beam density, the large energy loss of REB electron was observed after the beam pinch took place. In the case of a Ni coated polyethylene target, Ni plasma limits the region where the instability can grow to lower density due to large electron-ion collision, and the anomalous energy loss decreases.

In summary, the existence of the anomalous deposition of REB energy on a low- z target has been found experimentally. The experimental results show: (i) the energy loss of an electron transmitted through a polyethylene target was much larger than the stopping power estimated by coulomb scattering, and (ii) this large energy loss should be due to the kinetic two-stream instability in low- z corona plasma.

¹M.J. Clauser, Phys. Rev. Lett. **34**, 570 (1975).

²M.A. Sweeney, Appl. Phys. Lett. **29**, 231 (1976).

³K. Imasaki, S. Nakai, and C. Yamanaka, J. Phys. Soc. Jpn. **38**, 1554 (1975).

⁴S. Nakai, K. Imasaki, and C. Yamanaka, 6th International Conference on Plasma Physics and Controlled Nuclear Fusion, 1976 (unpublished).

⁵H. Azechi, H. Fujita, K. Imasaki, Y. Izawa, Y. Kato, Y. Kawamura, M. Matoba, K. Mima, S. Miyamoto, Y. Mizumoto, T. Mochizuki, S. Nakai, K. Nishihara, H. Nishimura, T. Norimatsu, T. Sasaki, H. Takabe, J.J. Thomson, K. Yoshida, T. Yamanaka, and C. Yamanaka, 7th International Conference on Plasma Physics and Controlled Nuclear Fusion, 1978 (unpublished).

⁶K. Imasaki, S. Miyamoto, S. Nakai, and C. Yamanaka, Tech. Rep. Osaka Univ. **27**, 165 (1977).

⁷J.M. Creedon, J. Appl. Phys. **46**, 2946 (1975).

⁸M.M. Widner and J.W. Poukey, Phys. Rev. Lett. **38**, 548 (1977).

⁹D. Mosher and I.B. Bernstein, Phys. Rev. Lett. **38**, 1483 (1977).

¹⁰E. Nardi, E. Peleg, and Z. Zinamon, Plasma Phys. **20**, 597 (1978).

¹¹K. Imasaki, S. Miyamoto, S. Nakai, and C. Yamanaka, J. Phys. Soc. Jpn. **40**, 1529 (1976).

Composition measurements related to the $\text{Cu}_2\text{S}/\text{Zn}_x\text{Cd}_{1-x}\text{S}$ heterojunction

L. C. Burton

Department of Electrical Engineering, Virginia Polytechnic Institute and State University, Blacksburg, Virginia 24061

(Received 26 July 1979; accepted for publication 29 August 1979)

Compositions of zinc and cadmium have been measured for three key regions related to the formation of Cu_2S on $\text{Zn}_x\text{Cd}_{1-x}\text{S}$ by aqueous ion exchange. These are the ion-exchange solution, the resulting Cu_2S , and the $\text{Zn}_x\text{Cd}_{1-x}\text{S}$ near the Cu_2S - $\text{Zn}_x\text{Cd}_{1-x}\text{S}$ interface. It is found that the participation of zinc in the ion-exchange reaction is incomplete. Zinc is thus retained in the p-n junction region, and is found mainly in the $\text{Zn}_x\text{Cd}_{1-x}\text{S}$ just under the interface. This phenomenon helps to account for certain differences between electro-optical properties of $\text{Cu}_2\text{S}/\text{CdS}$ and $\text{Cu}_2\text{S}/\text{Zn}_x\text{Cd}_{1-x}\text{S}$ solar cells.

PACS numbers: 73.40.Lq, 68.10. — m, 68.45. — v, 68.55. + b

The $\text{Cu}_2\text{S}/\text{Zn}_x\text{Cd}_{1-x}\text{S}$ solar cell is being developed because it offers a significantly higher voltage than that generated by the $\text{Cu}_2\text{S}/\text{CdS}$ junction. Higher open-circuit voltages for $\text{Cu}_2\text{S}/\text{Zn}_x\text{Cd}_{1-x}\text{S}$ junctions have been reported by several sources.¹⁻⁴ However, current densities are lower than for $\text{Cu}_2\text{S}/\text{CdS}$ cells made under similar conditions.

The $\text{Cu}_2\text{S}/\text{Zn}_x\text{Cd}_{1-x}\text{S}$ junction model is basically that of the $\text{Cu}_2\text{S}/\text{CdS}$, modified for changes in the $\text{Zn}_x\text{Cd}_{1-x}\text{S}$ band parameters.^{5,6} Differences between CdS and

$\text{Zn}_x\text{Cd}_{1-x}\text{S}$ based cells can be attributed to processes occurring in one or more of three cell regions: the Cu_2S , the interface, and the $\text{Zn}_x\text{Cd}_{1-x}\text{S}$. The Cu_2S is the absorbing region, whose properties could be modified when formed on $\text{Zn}_x\text{Cd}_{1-x}\text{S}$. At the interface, a potential energy spike could exist due to the decreased electron affinity of the $\text{Zn}_x\text{Cd}_{1-x}\text{S}$, with a resulting decrease in current density. The collection efficiency for electrons generated in the Cu_2S is determined in part by their mobility in the $\text{Zn}_x\text{Cd}_{1-x}\text{S}$, and

TABLE I. Cd and Zn masses for nominal 14% powder.

Solution	Cd (mg)	Zn (mg)	Zn/Cd
Pre-HCl	1.060	0.140	0.134
Cuprous ion	14.250	1.400	0.098
KCN	0.005	0.0135	2.700
Post-HCl	0.750	0.255	0.340
Bulk-HCl	22.150	2.990	0.135

by the electric field at the edge of the depletion layer, which lies almost entirely in the $Zn_x Cd_{1-x}S$. The properties of all of these regions could depend on the composition of the $Zn_x Cd_{1-x}S$.

In order to clarify causes for the differences between CdS and $Zn_x Cd_{1-x}S$ based cells, we have measured compositions near the interface by means of atomic absorption spectroscopy (AAS). The profiles of Zn and Cd in the Cu_2S and near the interface were of special interest.

Cu_2S layers were formed on both powders and films of $Zn_x Cd_{1-x}S$ by means of the aqueous ion-exchange process,⁷ which is diagrammed in Fig. 1. Cd and Zn concentrations were measured in the following solutions: initial HCl etch, the cuprous ion solution in which the Cu_2S was formed, the KCN solution in which the Cu_2S was removed, HCl etch following Cu_2S removal, and HCl etch of an identical $Zn_x Cd_{1-x}S$ sample to verify starting base composition.

Zn and Cd masses and the Zn/Cd ratio measured in the above five solutions for a nominal 14% (by weight) powder base are shown in Table I.

Concerning the data of Table I, the following points are of interest, and also pertain to other samples studied, both powders and films:

(1) The cuprous ion solution, in which the Cu_2S is formed, is deficient in zinc (compare the Zn/Cd ratio to that of the bulk). From this data, about 1.9 mg of Zn should be in the Cu^+ solution. Thus, roughly 0.5 mg of Zn is not accounted for.

(2) The Zn/Cd ratio in the Cu_2S significantly exceeds that of the base material, being greater than unity for several samples.

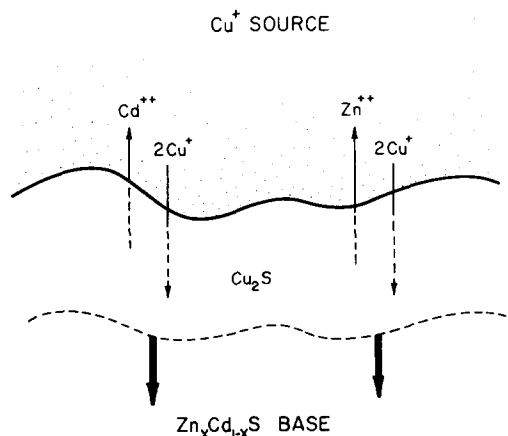


FIG. 1. Diagram of the ion-exchange system being studied.

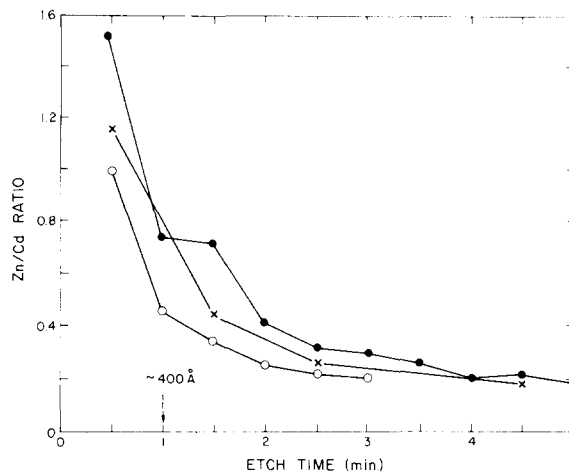


FIG. 2. Zn/Cd ratio as a function of etch time for $Zn_x Cd_{1-x}S$ region beneath the $Cu_2S-Zn_x Cd_{1-x}S$. Cu_2S formation time was 3 min, Cu_2S was removed in 0.1 M KCN; and the etch was 10% HCl (by volume) at room temperature.

(3) Amounts of Cd and Zn measured in the Cu_2S are less than $3 \times 10^{19} \text{ cm}^{-3}$ and $7 \times 10^{19} \text{ cm}^{-3}$, respectively, being $\leq 10^{19} \text{ cm}^{-3}$ for Cu_2S formed on thin films of $Zn_x Cd_{1-x}S$. These values are less than the copper vacancy concentration for $Cu_{1.995}S$ (chalcocite), which is about 10^{20} cm^{-3} .

(4) There is apparently excess Zn under the $Cu_2S-Zn_x Cd_{1-x}S$ interface (as measured in the post-HCl solution).

Zn profiles beneath the interface were obtained following Cu_2S removal, by successively etching away thin $Zn_x Cd_{1-x}S$ layers in dilute HCl. These results for three thin-film samples ($Zn/Cd \approx 0.20$ by weight) are shown in Fig. 2. The Zn content is seen to decrease to its bulk value over a distance of about 2000 Å (based on an average etch rate of 400 Å/min).

In order to verify that this excess Zn is not an etching artifact, layers of $Zn_x Cd_{1-x}S$ were removed in a similar

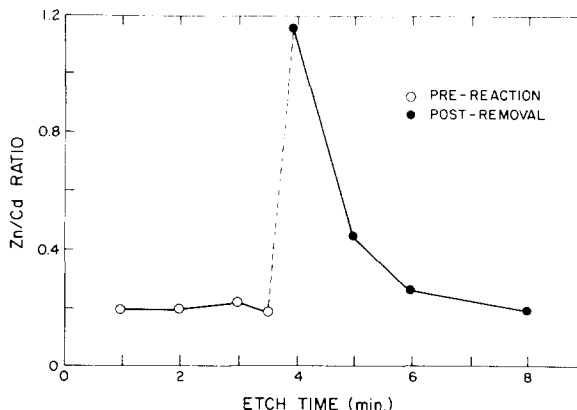


FIG. 3. Zn/Cd ratio versus etch time for a thin-film sample, before formation of the Cu_2S , and after its removal.

manner prior to Cu_2S formation. The measured Zn/Cd ratios, and those found subsequent to Cu_2S removal, are shown in Fig. 3. It is seen that the initial values are similar to the bulk values, indicating that a preferential etch phenomenon is not responsible for the enhanced Zn concentrations measured just under the interface.

About 75% of available Zn participates in the ion-exchange reaction and enters the cuprous ion solutions as Zn^{++} . The remaining 25% is retained in the p - n junction system. Our measurements indicate that only a small fraction of this is retained in the Cu_2S , with it mostly being detected below the interface in the $\text{Zn}_x\text{Cd}_{1-x}\text{S}$. This can be accounted for by low solubilities of Zn and Cd in Cu_2S (about $5 \times 10^{-19} \text{ cm}^{-3}$ or less) in addition to the diffusivity of Zn^{++} in Cu_2S being less than that of Cd^{++} .

The excess Zn found under the Cu_2S - $\text{Zn}_x\text{Cd}_{1-x}\text{S}$ interface could account for some of the differences between CdS and $\text{Zn}_x\text{Cd}_{1-x}\text{S}$ based solar cells. The actual $\text{Zn}_x\text{Cd}_{1-x}\text{S}$ composition under the interface differs from that of the starting film, and the cell model must be changed accordingly. Even for moderately low Zn content films, this phenomenon could result in a potential spike at the interface and/or reduced values of mobility and electric field, with a subsequent reduction in photogenerated current.

These results indicate that techniques other than ion-exchange might be necessary for Cu_2S formation on

$\text{Zn}_x\text{Cd}_{1-x}\text{S}$ films. However, if these phenomena are taken into account, and if appropriate changes can be made in the ion-exchange procedures, the net effect may not be detrimental.

Further studies are being conducted, including AAS and Auger/ESCA measurements, in an effort to clarify these points with more certainty. These results will be reported in a separate communication.

Acknowledgment is extended to Barbara Thomson and Judy Alls for performing the atomic absorption measurements.

¹W. Palz, J. Besson, T. Nguyen Duy, and J. Vedel, *Proceedings of the 10th Photovoltaic Specialists Conference, Palo Alto, Calif.* (IEEE, New York, 1973).

²T.M. Peterson, Ph.D. thesis, Lawrence Berkeley Laboratory, University of California at Berkeley, 1975.

³L.C. Burton and T.L. Hench, *Appl. Phys. Lett.* **29**, 612 (1976).

⁴S. Martinuzzi, J. Oualid, D. Sarti, and J. Gervais, *Thin Solid Films* **51**, 211 (1978).

⁵A. Rothwarf, Institute of Energy Conversion, University of Delaware Technical Report NSF/RANN/AER 72-03478 A03 TR 75/4, 1975.

⁶L.C. Burton, B. Baron, T.L. Hench, and J.D. Meakin, *J. Electron. Mater.* **1**, 159 (1978).

⁷L.R. Shiozawa, F. Augustine, G.A. Sullivan, J.M. Smith, III, and W.R. Cook, Jr., Aerospace Research Laboratories Report ARL 69-0155, 1969.

New experimental evidence of the periodic surface structure in laser annealing

M. Oron^{a)} and G. Sørensen

Institute of Physics, University of Aarhus, DK-8000 Aarhus C, Denmark

(Received 11 July 1979; accepted for publication 29 August 1979)

This letter presents a study of the nature of the periodic structure observed on the edge of laser-annealed spots on ion-implanted silicon. The direction of the periodic fringes was always found to be about perpendicular to the \mathbf{E} vector of the light for linearly polarized beams. No fringe pattern was observed for circular polarization. We suggest that the pattern observed is due to heating by a standing wave resulting from the interference of the impinging wave and a radial (longitudinal) scattered wave.

PACS numbers: 79.20.Nc, 79.20.Ds, 52.50.Jm, 85.30. — z

In recent years, pulsed lasers such as Nd glass and ruby have been used to anneal damage created by ion implantation in semiconductors.^{1,2} This technique may be of future technological importance since laser annealing has obvious advantages compared to conventional thermal annealing. Consequently, there has been a general interest in the interaction of a laser beam with plane solid surfaces. Some experimenters have reported on a formation of a periodic-surface

structure in ion-implanted semiconductors after laser annealing.^{3,4} The phenomenon of a surface-ripple structure visible in an optical microscope is related to the laser-surface interaction, and various models have been proposed to account for the observation. The present contribution deals with the formation of periodic surface structures around the laser spot in laser-annealed heavily krypton-doped silicon. Krypton was chosen as the dopant because when implanted with high doses, annealing at high temperatures causes bubble formation, and this will clearly reveal any lateral periodicity in the dopant distribution.

^{a)}Permanent address: Soreq Nuclear Research Centre, Yavne, Israel.